High-frequency field intensity along focal point of a long metallic parabolic reflector coated by a magnetized plasma layer using oblique incidence

Abdul Ghaffar[1,2,*] and Majeed A. S. Alkanhal[1]

[1]*Department of Electrical Engineering, King Saud University, Riyadh 11421, Saudi Arabia*
[2]*Department of Physics, University of Agriculture, Faisalabad 38040, Pakistan*
**Corresponding author: aghaffar@ksu.edu.sa*

Received February 11, 2015; accepted June 8, 2015; posted online July 21, 2015

Theoretical analysis of the electromagnetic field distribution in the focal region of a long metallic parabolic reflector that has its surface covered with a magnetized plasma layer is derived. The incident wave is considered to be with a general oblique incidence for both parallel and perpendicular polarizations. The electromagnetic field intensity expressions along the focal region are obtained accurately using Maslov's method. The effects of plasma thickness on the reflected and transmitted field distributions are investigated. The effects of other physical parameters such as the angle of incidence and the plasma and cyclotron frequencies on the transmitted field-intensity distribution along the focal region are also studied. The results obtained by Maslov's method and Kirchhoff's approximation are found to be in a good agreement.

OCIS code: 080.0080.
doi: 10.3788/COL201513.090801.

In current eras, the EM wave propagation in plasma attracted the scientists to explore new outcome on plasma-based reflector antenna, waveguides, and absorbers[1–5]. This noteworthy research works explored effects of plasma material on polarizations, beam patterns, efficiencies, and surface errors on these devices and their applications[6–8]. The study of focal point filed of parabolic reflector is significant for its uses in many areas of astronomy, communication, and medical field.

When space-based vehicle re-enters in space, the effects of plasma are noticeable which affect the performance of the instruments[9,10]. There are various types of geometry of reflectors have been examined for EM waves focusing[11,12]. Among the different-shaped reflectors, the parabolic reflector can be termed as the ideal focusing system. The main advantage of this reflector is that it focuses on a focal point for the parallel beam that hits on it and vice versa. The resulting reflected image is free of aberrations in geometrical optics (GO) approximation.

The reflected and the transmitted field intensities distribution from this parabolic reflector with its anisotropic plasma surface-layer along focal point using Maslov's method are presented in this Letter. This technique has been used successfully[13–17]. The effects of the plasma layer width and the plasma and cyclotron frequencies and the angle of incidence on the transmitted out intensity obtained at the focal point have been studied. To support the results of the presented formulations, Kirchhoff's approximation has been applied to the same problem and its results endorse the accuracy of the presented analysis. Solution by Maslov's method leads to a simple integral with a single variable, whereas the Kirchhoff's approximation needs Fresnel approximations. The time-harmonic ($j\omega t$) is considered and omitted throughout the Letter.

Consider a parabolic reflector made of a perfect electric material with an anisotropic plasma layer exposed to an external uniform magnetic field $\mathbf{B} = B_0\hat{e}_z$ as depicted in Fig. 1. The surface equation of the perfectly electrical conductive (PEC) parabolic reflector can be written as

$$\zeta = f - \xi^2/4f, \tag{1}$$

where f is the focal length of the reflector. The surface equation of the anisotropic plasma-layer-coated reflector can be written as

$$\zeta = f - d - \xi^2/4f, \tag{2}$$

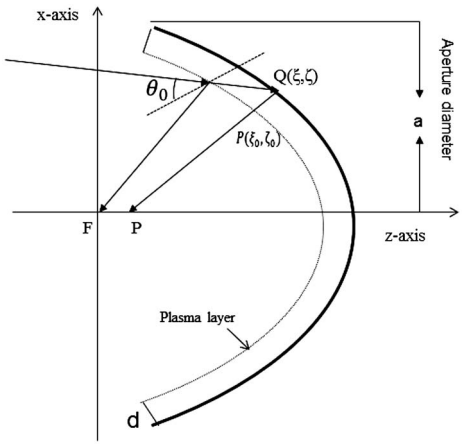

Fig. 1. Metallic parabolic reflector coated with a layer of magnetized plasma.

where d is the width of the coated layer. Let $P(\xi_0, \zeta_0)$ and $Q(\xi, \zeta)$ are the coordinate points on the PEC reflector and plasma layer parabolic surface, respectively. The relative permittivity tensor of anisotropic plasma layer[9,10] can be defined as

$$\bar{\bar{\varepsilon}} == \begin{vmatrix} \varepsilon_1 & -\mathrm{j}\varepsilon_2 & 0 \\ j\varepsilon_2 & \varepsilon_1 & 0 \\ 0 & 0 & \varepsilon_3 \end{vmatrix}, \tag{3}$$

where ε_1, ε_2, and ε_3 are defined in Refs. [9,10]. The wave numbers in anisotropic plasma for parallel and perpendicular polarization are defined as $k_1 = k_0/\sqrt{m}$, $k_2 = k_0/\sqrt{m_3}$, $m = \varepsilon_1/(\varepsilon_1^2 - \varepsilon_2^2)$, and $m_3 = 1/\varepsilon_3$, respectively. Consider an EM wave with parallel polarization incident with an oblique angle θ_0 on the plasma layer as

$$\begin{aligned} \mathbf{E_{0i}} = {} & E_i(\cos\theta_0 \hat{e}_x - \sin\theta_0 \hat{e}_z) \\ & \times \exp[-jk_i(x\sin\theta_0 + z\cos\theta_0)]. \end{aligned} \tag{4}$$

In the plasma layer, one is an extra ordinary wave propagate toward the border $z = \zeta$ and the other propagate toward the border $z = \zeta_0$. Using the following mathematical form of Snell's laws

$$\mathbf{p^r} = \mathbf{p^i} - 2(\mathbf{p^i} \cdot \mathbf{N})\mathbf{N}, \tag{5}$$

$$\mathbf{q^r} = \mathbf{p^i} + \sqrt{n^2 - 1 + (\mathbf{p^i} \cdot \mathbf{N})^2}\mathbf{N} - (\mathbf{p^i}.\mathbf{N})\mathbf{N}, \tag{6}$$

where $\mathbf{p^i}$ is the wave vector of the incident wave, n is refractive index of the anisotropic plasma medium, and $\mathbf{N}$ is the normal to the surface of the reflector coated with plasma layer which can be written as

$$\mathbf{N} = \hat{e}_z \cos\alpha + \hat{e}_x \sin\alpha. \tag{7}$$

The reflected wave vector $\mathbf{p}_1$ and refracted wave vector $\mathbf{q}_1$ of the plasma layer, respectively, are

$$\mathbf{p}_1 = -\hat{e}_x \sin(2\alpha - \theta_0) - \hat{e}_z \cos(2\alpha - \theta_0), \tag{8}$$

$$\begin{aligned} \mathbf{q}_1 = {} & \hat{e}_x(\sin\alpha(\mathrm{K}_1 - \cos(\alpha - \theta_0)) + \sin\theta_0) \\ & - \hat{e}_z(\cos\alpha(\mathrm{K}_1 - \cos(\alpha - \theta_0)) + \cos\theta_0). \end{aligned} \tag{9}$$

The reflected wave vector $\mathbf{p}_2$ from the metallic reflector and refracted wave vector $\mathbf{q}_2$ out of the layer respectively, for parallel polarization are

$$\begin{aligned} \mathbf{p}_2 = {} & -\hat{e}_x(\mathrm{K}_2 \sin\alpha + \cos\alpha \sin(\alpha - \theta_0)) \\ & - \hat{e}_z(\mathrm{K}_2 \cos\alpha + \sin\alpha \sin(\alpha - \theta_0)), \end{aligned} \tag{10a}$$

$$\begin{aligned} \mathbf{q}_2 = {} & -\hat{e}_x(\mathrm{K}_3 \sin\alpha + n_1 \cos\alpha \sin(\alpha - \theta)) \\ & - \hat{e}_z(\mathrm{K}_3 \cos\alpha + n_1 \sin\alpha \sin(\alpha - \theta)), \end{aligned} \tag{10b}$$

$$\begin{aligned} \mathrm{K}_1 &= \sqrt{n_1^2 - \sin^2(\alpha - \theta_0)}, \\ \mathrm{K}_2 &= \sqrt{n_1^2 + \cos(2\alpha - 2\theta_0) - 1)/2}, \\ n_1 &= \sqrt{(\varepsilon_1^2 - \varepsilon_2^2)/\varepsilon_1}, \\ \mathrm{K}_3 &= \sqrt{(\Gamma + (\cos(2\alpha - 2\theta_0) - 1 + 2n_1^2)n_1)/2}, \\ \Gamma &= 2(\varepsilon_1 - \varepsilon_1^2 - \varepsilon_2^2)/\varepsilon_1. \end{aligned} \tag{11}$$

Consider an electromagnetic wave perpendicularly polarized obliquely incident with an angle θ_0 on the parabolic anisotropic plasma layer as

$$\mathbf{E_{0i}} = E_i \hat{e}_y \exp[-jk_i(x\sin\theta_0 + z\cos\theta_0)]. \tag{12}$$

The refracted wave vector $\mathbf{q}_3$ into the layer, the reflected wave vectors $\mathbf{p}_3$, and the refracted wave vector $\mathbf{q}_4$ of out of the plasma layer, respectively, into free space for perpendicular polarization are

$$\mathbf{q}_3 = \hat{e}_x(\sin\alpha(\sin\theta_0 - \mathrm{K}_4)) - (\cos\alpha(\cos\theta_0 - \mathrm{K}_4))\hat{e}_z, \tag{13a}$$

$$\begin{aligned} \mathbf{p}_3 = {} & -\hat{e}_x(\mathrm{K}_5 \sin\alpha + \cos\alpha \sin(\alpha - \theta_0)) \\ & - \hat{e}_z(\mathrm{K}_5 \cos\alpha + \sin\alpha \sin(\alpha - \theta_0)), \end{aligned} \tag{13b}$$

$$\begin{aligned} \mathbf{q}_4 = {} & \hat{e}_x(\mathrm{K}_6 \sin\alpha + n\cos\alpha \sin(\theta - \alpha)) \\ & - \hat{e}_z(\mathrm{K}_6 \cos\alpha + n\sin\alpha \sin(\alpha - \theta)), \end{aligned} \tag{14}$$

$$\begin{aligned} \mathrm{K}_4 &= \cos(\alpha - \theta_0) - \sqrt{n^2 - \sin^2(\alpha - \theta_0)}, \\ \mathrm{K}_5 &= \sqrt{(-1 + 2n^2 + \cos(2\alpha - 2\theta))/2}, \\ \mathrm{K}_6 &= \sqrt{(2 - n - 2n^2 + 2n^3 + n\cos(2\alpha - 2\theta))/2}. \end{aligned} \tag{15}$$

Hamilton's equations are given by

$$\begin{aligned} & \mathrm{d}x/\mathrm{d}\tau = \mathrm{p}_x, \qquad \mathrm{d}z/\mathrm{d}\tau = \mathrm{p}_z, \qquad \mathrm{dp}_x/\mathrm{d}\tau = 0, \\ & d\mathrm{p}_z/\mathrm{d}\tau = 0. \end{aligned} \tag{16}$$

The solutions of the Hamilton's equations are

$$\begin{aligned} & x = \xi_0 + \mathrm{p}_{1x}\tau_1, \qquad z = \zeta_0 + \mathrm{p}_{1z}\tau_1, \\ & p_1 x = p_1 x^0, \qquad p_1 z = p_1 z^0, \end{aligned} \tag{17}$$

$$\begin{aligned} & x = \xi_0 + \mathrm{q}_{1x}\tau_1, \qquad z = \zeta_0 + \mathrm{q}_{1z}\tau_1, \\ & q_1 x = q_1 x^0, \qquad q_1 z = q_1 z^0. \end{aligned} \tag{18}$$

The Jacobians associated with waves reflected and refracted by the parabolic plasma layer are obtained

$$\mathrm{J}_1(\tau_1) = \frac{\mathrm{D}_1(\tau_1)}{\mathrm{D}_1(0)} = 1 - \frac{\tau_1 \cos^3\alpha}{f\cos(\alpha - \theta_0)}, \tag{19}$$

$$\mathrm{J}_2(\tau_2)=\frac{\mathrm{D}_2(\tau_2)}{\mathrm{D}_2(0)}=\frac{1}{8f\mathrm{K}_2^2}\{8f\mathrm{K}_1^2+\tau_2\cos^3\alpha \times[-2\mathrm{K}_1(2\mathrm{K}_1^2+n^2)-n(4\mathrm{K}_1^2+n) \times\cos(\alpha-\theta_0)+\cos(3\alpha-3\theta_0)]\}. \quad (20)$$

The GO fields' expressions for the reflected and transmitted rays out of the anisotropic plasma layer

$$E_r(x,z)=E_i[\mathrm{J}_1(\tau_1)]^{-\frac{1}{2}}\exp[-jk(\Psi_0+\tau_1)], \quad (21)$$

$$E_t(x,z)=E_i[\mathrm{J}_2(\tau_2)]^{-\frac{1}{2}}\exp[-jk(\Psi_0+\tau_2+t)], \quad (22)$$

where $\Psi_0=\xi_0\sin\theta_0+\zeta_0\cos\theta_0$, τ_1 and τ_2 are factors along the reflected and transmitted rays, respectively, and t is the length between the $P(\xi_0,\zeta_0)$ and $Q(\xi,\zeta)$. The GO fields become singular around the focal regions when $\mathrm{J}(\tau)=0$. The finite field expression by Maslov's method is as

$$\mathbf{E^r}(r)=\sqrt{\frac{k}{j2\pi}}\int_{-\infty}^{\infty}\mathbf{E_t}(x,z)\left[\frac{D(\tau)}{D(0)}\frac{\partial(\mathrm{p}_z)}{\partial(z)}\right]^{-\frac{1}{2}} \times\exp(-jk(S_0+\tau-z(p_x,z)p_z+p_zz))\mathrm{d}p_z. \quad (23)$$

Integrands of the reflected and the transmitted waves are

$$\mathrm{I}_1=\frac{D(\tau_1)}{D(0)}\frac{\partial(\mathrm{p}_{1x})}{\partial(x)}=-\frac{\sin^2(2\alpha-\theta_0)\cos^3\alpha}{f\cos(\alpha-\theta_0)}, \quad (24)$$

$$\mathrm{I}_2=\frac{D(\tau_2)}{D(0)}\frac{\partial(\mathrm{p}_{3x})}{\partial(x)}=\frac{4\mathrm{K}_2^2\sin\alpha}{8f\mathrm{K}_2^2\sec^3\alpha(\mathrm{K}_2\sin\alpha+n_1\cos\alpha\sin(\alpha-\theta_0))} +\frac{4\mathrm{K}_2^2\sin\alpha+n_1(\sin(\alpha-2\theta_0)+\sin(3\alpha-2\theta_0)+4\mathrm{K}_2\sin2\alpha-\theta_0)}{8f\mathrm{K}_2^2\sec^3\alpha(\mathrm{K}_2\sin\alpha+n_1\cos\alpha\sin(\alpha-\theta_0))}. \quad (25)$$

The phase functions for the both waves integrals are obtained, respectively, as

$$S_1=-2r\cos(\alpha-\theta_0)/\cos\alpha+\cos(2\alpha-\theta_0-\theta), \quad (26)$$

$$S_2=f\mathrm{K}_2\sec\alpha-\mathrm{K}_2r\cos(\alpha+\theta)+a\cos\alpha +t+f/2((2-n_1)\cos(2\alpha-\theta_0)+n_1\cos\theta_0)\sec^2\alpha +n_1r\sin(\alpha+\theta)\sin(\alpha-\theta_0)). \quad (27)$$

The initial value of the reflected field is defined as

$$\mathbf{E_r}(x,z)=-\mathbf{E_i}-2(\mathbf{E_i}\cdot\mathbf{N})\mathbf{N}. \quad (28)$$

Using Eqs. (24), (26), and (28) into Eq. (23) and changing the variable p_{1z} to α given in Eq. (8) yields the final reflected field expression components as

$$\frac{E_x(x,z)}{E_i}=-\sqrt{\frac{2kf}{\pi_i}}\int_{-l/2}^{l/2}\cos\theta_0\sqrt{\frac{\cos(\alpha-\theta_0)}{\cos^3\alpha}}\exp(-jkS_1)\mathrm{d}\alpha, \quad (29)$$

$$\frac{E_z(x,z)}{E_i}=-\sqrt{\frac{2kf}{\pi_i}}\int_{-l/2}^{l/2}\sin\theta_0\sqrt{\frac{\cos(\alpha-\theta_0)}{\cos^3\alpha}}\exp(-jkS_1)\mathrm{d}\alpha. \quad (30)$$

The initial value of the transmitted field is defined as

$$\mathbf{E_t}(x,z)=\tilde{T}\cdot\mathbf{E_i}==[T_\parallel\mathbf{i}_\parallel^t\mathbf{i}_\parallel^i+T_\perp\mathbf{i}_\perp^t\mathbf{i}_\perp^i]\cdot\mathbf{E_i}, \quad (31)$$

where $\mathbf{i}_\perp^i=\frac{\mathbf{P^i}\times\mathbf{n}}{|\mathbf{P^i}\times\mathbf{n}|}=\hat{e}_y$, $\mathbf{i}_\parallel^i=\mathbf{i}_\perp^i\times\mathbf{P^i}$, $\mathbf{i}_\perp^t=\frac{\mathbf{q^i}\times\mathbf{n}}{|\mathbf{q^i}\times\mathbf{n}|}=\hat{e}_y$, $\mathbf{i}_\parallel^t=\mathbf{i}_\perp^i\times\mathbf{q^i}$, $T_\parallel=\frac{2n_1\cos\alpha}{\cos\alpha+n_1\sqrt{1-n_1^2\sin^2\alpha}}$, and $T_\perp=\frac{2n_1\cos\alpha}{n_1\cos\alpha+\sqrt{1-n_1^2\sin^2\alpha}}$.

Again using Eqs. (25), (27), and (28) into Eq. (24) and changing the variable p_{2z} to α given in Eq. (10b) yields the transmitted field expression in components form

$$\frac{E_x(x,z)}{E_i}=\sqrt{\frac{2kf}{\pi}}\int_{-l/2}^{l/2}E_{tx}\sqrt{\frac{\mathrm{K}_3}{\cos^3\alpha\mathrm{q}_{2x}}\frac{d\mathrm{q}_{2\alpha}}{d\alpha}}\exp(-jkS_2)\mathrm{d}\alpha, \quad (32a)$$

$$\frac{E_z(x,z)}{E_i}=\sqrt{\frac{2kf}{\pi}}\int_{-l/2}^{l/2}E_{tz}\sqrt{\frac{\mathrm{K}_3}{\cos^3\alpha\mathrm{q}_{2x}}\frac{d\mathrm{q}_{2\alpha}}{d\alpha}}\exp(-jkS_2)\mathrm{d}\alpha, \quad (32b)$$

$$E_{tx}=\frac{2n_1\cos\alpha\cos2\theta_0(-\mathrm{K}_2\cos\alpha+n_1^2\sin\alpha\sin(\alpha-\theta_0)}{n_1\cos\alpha+\sqrt{1-n_1^2\sin^2\alpha}},$$

$$E_{tz}=\frac{2n_1\cos\alpha\cos2\theta_0(-\mathrm{K}_2\cos\alpha+n_1^2\cos\alpha\sin(\alpha-\theta_0)}{n_1\cos\alpha+\sqrt{1-n_1^2\sin^2\alpha}}. \quad (33)$$

The final reflected field expression for perpendicular polarization may be obtained as

$$E(x,z)/E_i=-\sqrt{2kf/\pi_i}\int_{-l/2}^{l/2}\sqrt{\cos(\alpha-\theta_0)/\cos^3\alpha} \times\exp(-jkS_1)\mathrm{d}\alpha. \quad (34)$$

Again using Eqs. (19) and (21) into Eq. (24) and changing the variable p_{2z} to α given in Eq. (10a) yields the final

finite transmitted field expression valid along the focal region as

$$\frac{E_y(x,z)}{E_i} = \sqrt{\frac{ka}{\pi}} \int_{-l/2}^{l/2} \frac{2n\cos\alpha}{n\cos\alpha + \sqrt{1-n^2\sin^2\alpha}} \times \sqrt{\frac{1}{q_{2x}} \frac{dq_{2z}}{d\alpha} \frac{K_2}{\cos^3\alpha}} \exp(-jkS_3)d\alpha, \quad (35)$$

where $S_3 = fK_3\sec\alpha - K_3 r\cos(\alpha+\theta) + a\cos\alpha + t + f((2-\sqrt{\epsilon_3})\cos(2\alpha-\theta_0) + \sqrt{\epsilon_3}\cos\theta_0)\sec^2\alpha + \sqrt{\epsilon_3} r\sin(\alpha+\theta s)\ln(\alpha-\theta_0))/2$, and l is the angle which reflector subtend with aperture diameter. To validate the aforementioned formulations, the fields expressions are obtained using the following formula implied by the Huygens–Kirchhoff's Integral (HKI)[16]

$$E(x,z) = \sqrt{\frac{k}{j2\pi}} \int_{-\infty}^{\infty} \frac{e^{-jR}}{R} E_0(\xi_0,\zeta_0)\exp(-jkS_0)d\xi_0, \quad (36)$$

where

$$R = q_{1x}(x-\xi_0) + q_{1z}(z-\zeta_0) = \sqrt{(x-\xi_0)^2 + p^2},$$
$$E_0 = J^{-\frac{1}{2}}.$$

The reflected and transmitted perpendicularly polarized electromagnetic wave, due to an oblique incident plane wave by a parabolic metal reflector with an anisotropic plasma layer on its surface, are obtained numerically. First, the results are compared with the HKI to check the correctness of the analytical expressions and numerical results as shown in Fig. 2 which are in good agreement. It is assumed that $\omega = 3.14 \times 10^8$ Hz, $kf = 12$, $\theta_0 = 1°$, $\omega_p = 1.7829 \times 10^8$ Hz, and $\omega_c = 1.3 \times 10^8$ Hz throughout the analysis. Figure 3 illustrates the reflected field intensity distribution from the parabolic reflector in presence of the anisotropic plasma layer along the focal points with respect to kz, for different plasma layer thickness values. From Fig. 3, it is observed that the reflected field intensity for both parallel and perpendicular

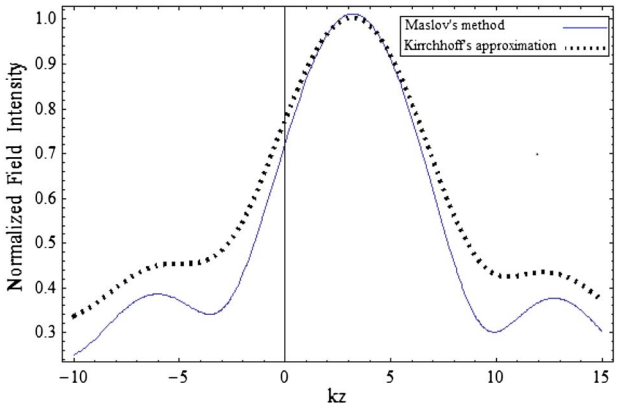

Fig. 2. Comparison of normalized results obtained by Maslov's method and HKI.

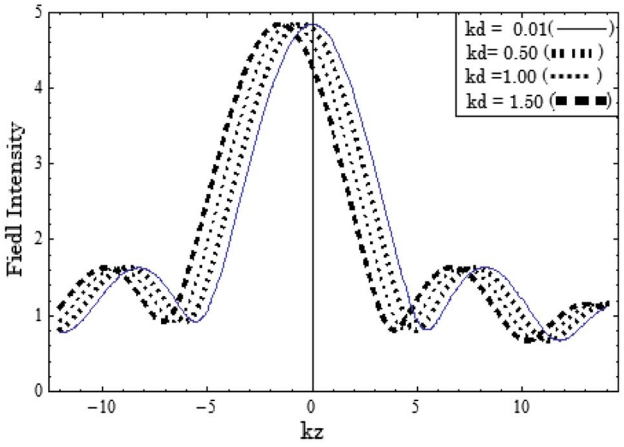

Fig. 3. Reflected wave field intensities distribution for different values of kd versus kz.

polarization is higher at lower values of the layer thicknesses. It is also observed that the location of the maximum reflected field intensity is displaced along the z-axis away from the reflector curved-surface at higher values of the layer thickness but retains the same magnitude. Figures 4(a) and 4(b) shows a comparison of the transmitted field intensity distribution from the parabolic reflector in the presence of the anisotropic layer along the focal points with respect to kz for parallel polarization and perpendicular polarization, respectively. The transmitted field intensity is higher at higher values of the plasma layer thickness. The transmitted field intensity is the same in

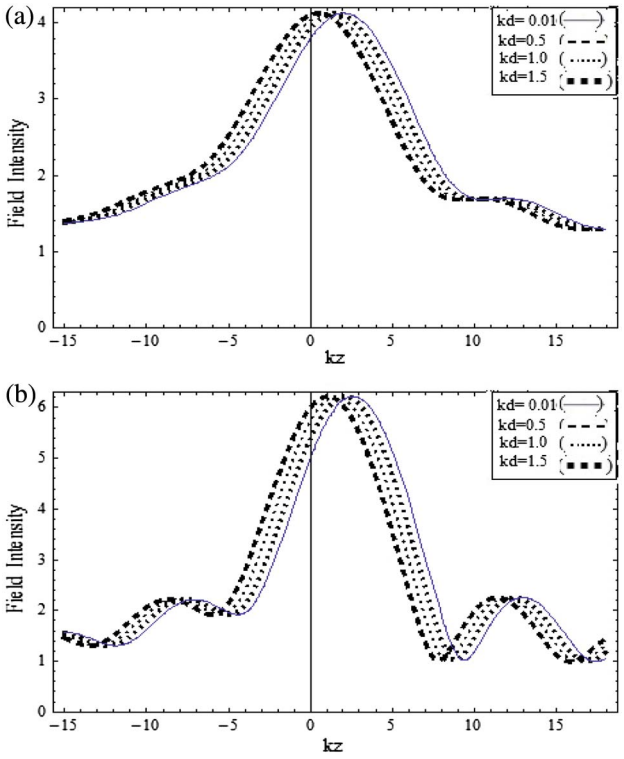

Fig. 4. Transmitted wave field intensities versus kz for different values of kd: (a) TE and (b) TM polarized.

magnitude but with some displacement away from the reflector curved-surface along the z-axis at higher values of the anisotropic plasma layer thickness. It is also observed that the field intensity of the perpendicular polarization incident wave is higher than the parallel polarization incident wave.

Figures 5–7 demonstrate, respectively, the effects of the plasma frequency, angle of incidence, and cyclotron frequency on the transmitted field distribution from the anisotropic plasma layer. Figures 5(a) and 5(b) show the transmitted field intensity versus kz for different values of the anisotropic plasma frequency ω_p with parallel polarization and the perpendicular polarization incident wave. Figures 5(a) and 5(b) have been plotted for a constant focal length of the metallic parabolic reflector at $kd = 0.5$. It is clearly observed that if the frequency of the plasma layer increases, the value of the transmitted field intensity decreases and the location of the maximum transmitted field intensity shifts away from the reflector for both polarized cases.

Figures 6(a) and 6(b) show the changes of the transmitted field intensity versus kz, for different values of the angle of incidence θ_0 of the incoming wave at $kd = 0.5$. As expected, if the incoming-wave angle of the incidence θ_0 increases, the value of the transmitted field intensity decreases.

Figure 7 represents the variations of the transmitted field intensity versus kx and kz for the parallel polarization incident waves at different values of the cyclotron frequency ω_c at $kd = 0.5$. If the cyclotron frequency ω_c increases, the value of the transmitted field intensity decreases along the x-axis and a shift of the location of the maximum transmitted field intensity towards the curved reflector interface for both polarized cases.

This Letter represents theoretical and numerical analyses of the EM fields in the focal point of a long metallic parabolic reflector coated with anisotropic plasma layer using both parallel and perpendicular polarization wave incidence with a general oblique incidence angle. Analytical field expressions along the focal line are derived using Maslov's method. The reflected and the transmitted field

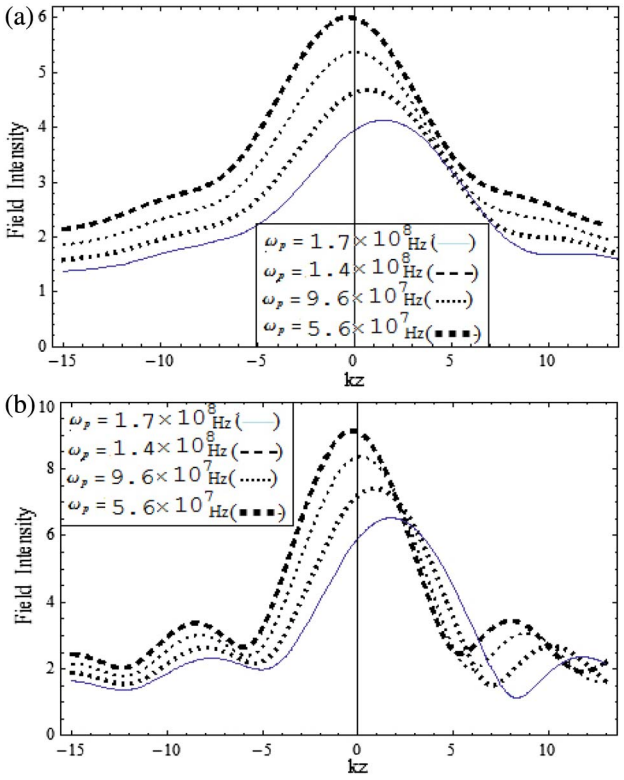

Fig. 5. Transmitted wave field intensities versus kz for different values of ω_p: (a) TE and (b) TM polarized.

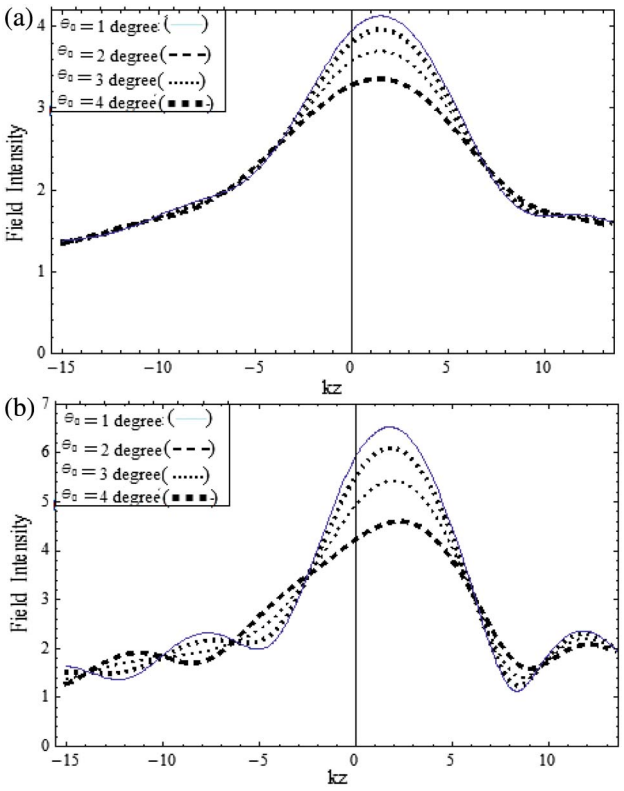

Fig. 6. Transmitted wave field intensities versus kz different values of θ_0: (a) TE and (b) TM polarized.

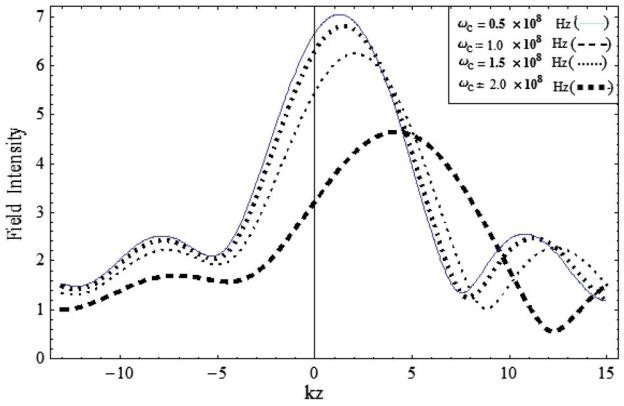

Fig. 7. Transmitted wave field intensities versus kz for different values of ω_c for TE polarized.

intensities from the anisotropic plasma layer are found to be in a good agreement to those obtained using HKI. The effects of the anisotropic plasma layer width, the plasma frequency, the cyclotron frequency on the transmitted, and the reflected intensities distribution are examined. The focal point is moved away from the reflector surface along the z-axis at higher values of the plasma layer width. When the plasma frequency and cyclotron frequency increase, the highest value of the transmitted field intensity decrease while the location of the focal point shifts closer to the reflector along the z-axis.

The authors would like to extend their sincere appreciation to the Deanship of Scientific Research at King Saud University for its funding of this work through the Research Group Project No. RG-1436-001.

References

1. D. R. Nicholson, *Introduction to Plasma Theory* (Wiley, 1983).
2. S. Yi, B. Mu, X. Wang, J. Zhu, L. Jiang, Z. Wang, and P. He, Chin. Opt. Lett. **12**, 013401 (2014).
3. K. Nakajima, H. T. Kim, T. M. Jeong, and C. H. Nam, High Power Laser Sci. Eng. **3**, e10 (2015).
4. C. S. Gurel and E. Oncu, Prog. Electromagnet. Res. B **21**, 385 (2010).
5. A. Niknam, M. Khajehmirzaei, B. Davoudi–Rahaghi, Z. Rahmani, B. Jazi, and A. Abdoli-Arani, Phys. Plasmas **21**, 073107 (2014).
6. G. Kuz'min, I. Minaev, K. Rukhadze, V. Tarakanov, and O. Tikhonevich, J. Commun. Technol. Electron. **57**, 536 (2012).
7. T. Anderson, *Plasma Antennas* (Artech House, 2011).
8. V. Smilyanskii, J. Appl. Mech. Technol. Phys. **12**, 366 (1971).
9. A. Ghaffar, M. Yaqoob, M. A. Alkanhal, M. Sharif, and Q. Naqvi, AEU-Int. J. Electron. Commun. **68**, 767 (2014).
10. B. Jazi, B. Davoudi-Rahaghi, M. R. Khajehmirzaei, and A. R. Niknam, IEEE Trans. Plasma Sci. **42**, 286 (2014).
11. T. Ma, X. Yuan, W. Ye, W. Xu, S. Qin, and Z. Zhu, Chin. Opt. Lett. **12**, 020501 (2014).
12. J. Hao, Z. Yu, Z. Chen, H. Chen, and J. Ding, Chin. Opt. Lett. **12**, 090501 (2014).
13. R. W. Ziolkowski and G. A. Deschamps, Radio Sci. **19**, 1001 (1984).
14. K. Hongo, Y. Ji, and E. Nakajima, Radio Sci. **21**, 911 (1986).
15. K. Hongo and Y. Ji, Radio Sci. **22**, 357 (1987).
16. A. Ghaffar, M. Sharif, Q. Naqvi, M. Alkanhal, F. Khalid, and S. Shukurullah, Appl. Comput. Electromagn. Soc. J. **29**, 478 (2014).
17. A. Ghaffar, M. Arif, Q. A. Naqvi, and M. A. Alkanhal, Optik-Int. J. Light Electron. Opt. **125**, 1589 (2014).